EFFECTS OF STANDARD AND PHOTOACTIVATED PLATELET-RICH PLASMA ON HUMAN MENISCUS FIBROCHONDROCYTES IN IL-1β-INDUCED INFLAMMATION

Kerimov KB[1], Ivanov AS[1,2,3] ✉, Tananakina TP[3], Kashchenko SA[3], Pogorelova IA[3]

[1] MEDSI Clinic, Clinical Hospital No. 1, Moscow, Russia
[2] Scientific and Diagnostic Center "Polyclinic on Smolenskaya", Moscow, Russia
[3] St. Luke Lugansk State Medical University, Russia

The meniscus degeneration pathogenesis is important for understanding and developing new treatment methods; it includes biochemical, structural, and microcirculatory alterations affecting all joint structures. The study aimed to perform *in vitro* assessment of the effects of standard and photoactivated platelet-rich plasma (PRP) on the IL6, IL17A concentrations, expression of COL2A1 and CD95 apoptosis marker in human meniscus fibrochondrocytes in the IL1β-induced inflammation. The human knee meniscus cartilage tissue was collected from 12 somatically healthy donors aged 18 to 35 years for the experiment. Cells were divided into four groups: the first was intact (control), the second, third, and fourth ones were exposed to IL1β to induce degenerative alterations; the second one was supplemented with 0.9% NaCl, the third one with donor PRP, and the fourth one with photoactivated PRP. Parameters were determined after 48 h. Statistical analysis was performed in GraphPad Prism 9. The rm-ANOVA was used for related groups. Data were presented as mean ± SD, at $p < 0.05$. IL6 (79.6 ± 4.3 pg/mL vs. 28.4 ± 2.1 pg/mL), IL17A (42.8 ± 2.5 pg/mL vs. 14.2 ± 1.0 pg/mL), CD95 (28.5 ± 2.2% vs. 6.8 ± 0.7%) levels increased in group II compared to group I; COL2A1 levels decreased from 1.00 ± 0.08 to 0.42 ± 0.5. IL6 levels decreased to 55.1 ± 3.4 pg/mL, IL17A — to 29.4 ± 2.1 pg/mL, CD95 — to 17.2 ± 1.5%, and COL2A1 levels increased to 0.71 ± 0.06 in group III compared to group II. IL6 levels decreased to 38.2 ± 2.6 pg/mL, IL17A — to 18.6 ± 1.7 pg/mL, CD95 — to 9.4 ± 0.8%, and COL2A1 levels increased to 0.94 ± 0.07 ($p < 0.05$) in group IV compared to group III. Standard PRP has a positive effect on meniscus tissue *in vitro* after 48 h. The effect is enhanced after the PRP exposure to red light.

Keywords: meniscus, fibrochondrocytes, platelet-rich plasma, PRP, photoactivation, red light, interleukin, COL2A1, CD95

Author contribution: Kerimov KB — study design, experimental procedure, calculations; Ivanov AS — study design, experimental design; Tananakina TP — study design, experimental design, scientific supervision; Kashchenko SA — scientific editing, scientific supervision, part in preparing the experiment; Pogorelova IA — technical proofreading, part in preparing the experiment.

Compliance with ethical standards: the study approved by the Ethics Committee of the St. Luke Lugansk State Medical University (protocol No. 2 dated May 26, 2026) was fully compliant with the Eurasian Economic Commission (EEC) Board "Guidelines for the Use of Laboratory (Experimental) Animals in Preclinical (Non-Clinical) Studies" dated November 14, 2023, No. 33, principles of the European Convention for the Protection of Vertebrate Animals used for Experimental and Other Scientific Purposes, as well as the Directive of the European Parliament and of the Council of the European Union on the Protection of Animals Used for Scientific Purposes. All the patients submitted the written informed consent for the material collected to be used for experimental purposes.

✉ **Correspondence should be addressed:** Aleksey S. Ivanov
A. Dikogo 16A, 73, 111396, Moscow, Russia, sashatravmatolog1985@mail.ru

Received: 27.06.2026 **Accepted:** 20.08.2026 **Published online:** 26.08.2026

DOI: 10.24075/brsmu.2026.046

ВЛИЯНИЕ СТАНДАРТНОЙ И ФОТОАКТИВИРОВАННОЙ ОБОГАЩЕННОЙ ТРОМБОЦИТАМИ ПЛАЗМЫ НА ФИБРОХОНДРОЦИТЫ МЕНИСКА ЧЕЛОВЕКА ПРИ IL1β-ИНДУЦИРОВАННОМ ВОСПАЛЕНИИ

К. Б. Керимов[1], А. С. Иванов[1,2,3] ✉, Т. П. Тананакина[3], С. А. Кащенко[3], И. А. Погорелова[3]

[1] Клиника «МЕДСИ», Клиническая больница № 1, Москва, Россия
[2] Научно-диагностический центр «Поликлиника на Смоленской», Москва, Россия
[3] ФГБОУ ВО ЛГМУ имени Святителя Луки Минздрава России, Россия

Патогенез дегенеративных изменений мениска важен для понимания и разработки новых методик лечения и включает в себя биохимические, структурные и микроциркуляторные изменения, затрагивающие все структуры сустава. Цель исследования — изучить влияние стандартной и фотоактивированной обогащенной тромбоцитами плазмы (PRP) *in vitro* на концентрацию IL6, IL17A, экспрессию COL2A1 и маркера апоптоза CD95 фиброхондроцитов мениска человека при IL1β-индуцированном воспалении. Для эксперимента отобрали хрящевую ткань мениска коленного сустава человека у 12 соматически здоровых доноров от 18 до 35 лет. Клетки разделены на четыре группы: первая — интактная (контроль), вторая, третья и четвертая подвергались воздействию IL1β для индукции дегенеративных изменений, во вторую вносили 0,9% NaCl, в третью — PRP доноров, в четвертую — PRP с фотоактивацией. Показатели определяли через 48 ч. Статистические расчеты проводили в GraphPad Prism 9. Для связанных групп применяли rm-ANOVA. Данные представлены как mean ± SD, при $p < 0,05$. Во II группе в сравнении с I возрастали IL6 (79,6 ± 4,3 пг/мл против 28,4 ± 2,1 пг/мл), IL17A (42,8 ± 2,5 пг/мл против 14,2 ± 1,0 пг/мл), CD95 (28,5 ± 2,2% против 6,8 ± 0,7%) соответственно; снизился COL2A1 (с 1,00 ± 0,08 до 0,42 ± 0,05); в III группе по сравнению со II снижались IL6 до 55,1 ± 3,4 пг/мл, IL17A — до 29,4 ± 2,1 пг/мл, CD95 до 17,2 ± 1,5%, COL2A1 повысился до 0,71 ± 0,06; IV группе по сравнению с III снижались IL6 до 38,2 ± 2,6 пг/мл, IL17A — до 18,6 ± 1,7 пг/мл, CD95 — до 9,4 ± 0,8%; повысился COL2A1 до 0,94 ± 0,07 ($p < 0,05$). Стандартная PRP оказывает положительное влияние на ткани мениска *in vitro* через 48 ч. Эффект усиливается после воздействия красного света на PRP.

Ключевые слова: мениск, фиброхондроциты, обогащенная тромбоцитами плазма, PRP, фотоактивация, красный свет, интерлейкин, COL2A1, CD95

Вклад авторов: К. Б. Керимов — дизайн исследования, экспериментальная часть работы, расчеты; А. С. Иванов — дизайн исследования, экспериментальная часть работы; Т. П. Тананакина — дизайн исследования, экспериментальная часть работы, научное сопровождение; С. А. Кащенко — научное редактирование, научное сопровождение, подготовка эксперимента; Погорелова И. А. — техническое редактирование, подготовка эксперимента.

Соблюдение этических стандартов: исследование одобрено этическим комитетом ФГБОУ ВО ЛГМУ имени Святителя Луки, МЗ РФ (протокол № 2 от 26 мая 2026 г.), полностью соответствует рекомендации Коллегии ЕЭК «Руководство по работе с лабораторными (экспериментальными) животными при проведении доклинических (неклинических) исследований от 14.11.2023 № 33», принципам Европейской конвенции о защите позвоночных животных, используемых для экспериментов или в иных научных целях, а также в соответствии с директивой Европейского парламента и совета Европейского союза по охране животных, в научных целях. Все пациенты подписали письменное согласие на использование полученного материала для экспериментальных целей.

✉ **Для корреспонденции:** Алексей Сергеевич Иванов
ул. А. Дикого, д. 16А, кв. 73, 111396, г. Москва, Россия, sashatravmatolog1985@mail.ru

Статья получена: 27.06.2026 **Статья принята к печати:** 20.08.2026 **Опубликована онлайн:** 26.08.2026

DOI: 10.24075/vrgmu.2026.046

Musculoskeletal disorders with the human knee meniscus degenerative-dystrophic alterations affect a broad segment of the population, primarily people of working age, and often become the cause of disability, which determines the medical, social and economic burden for each patient and society as a whole [1]. The meniscus tissue degeneration pathogenesis includes biochemical, structural, and microcirculatory alterations affecting all joint structures, and understanding the pathogenesis is important for the development of new treatment methods [2]. The cartilage degeneration results from the combined effects of biological and mechanical factors leading to violation of the joint homeostasis, subsequent development of persistent inflammation with the increase in pro-inflammatory cytokine concentrations, initiation of apoptotic processes, downregulation of the genes encoding the extracellular matrix components, and, finally, to the cartilage tissue volume reduction and the joint biomechanics alteration [3].

Pro-inflammatory cytokines (IL1β, IL6, IL8, IL17A, and tumor necrosis factor) play a significant role in the development of progression of the meniscus tissue degeneration. IL1β causes inhibition of the new collagen and proteoglycan synthesis in chondrocytes, including due to activation of metalloproteinase enzymes. The tumor necrosis factor induces local synovial membrane inflammation and chondrocyte apoptosis in the joint. IL8 causes the recruitment of immune cells (neutrophils and macrophages) into the joint cavity, thereby increasing damage [4]. IL6 is known not only as an inflammation development and progression factor; its physiological effects are of great importance. It is produced by T and B cells, granulocytes, smooth muscle cells, eosinophils, mast cells, glial cells, keratocytes; it is involved in the endocrine, hematopoietic, nervous system functioning [5]. In previous *in vitro* studies, the IL6 capability of inducing inhibitors of matrix metalloproteinases was determined [6]. The increase in the synovial fluid cytokine concentrations leads to increased pain and loss of cartilage tissue volume, especially in end-stage osteoarthritis [1, 7]. It has been shown that in patients with the combination of obesity and osteoarthritis, blood levels of IL6 are elevated and correlation with the progression of these disorders [8].

IL17A plays an important role in the pathogenesis of the knee meniscus tissue degeneration. The cytokine is produced by macrophages, as well as by the γδ–T cells that are found in mucous membranes and involved in antimicrobial immunity. It is assumed that these cells contribute to bone tissue regeneration. In individuals with the knee meniscus tissue degeneration, γδ–T cells can cause the increased interleukin production on a par with NK cells, the synovial membrane counts of which are increased in osteoarthritis [9]. NK cells accumulate in inflamed tissues, where these are stimulated by other pro-inflammatory cytokines (IL12, IL15, and IL18) secreted by monocytes. Suppression of anabolic factors (for example, downregulation of the COL2A1 gene) in chondrocytes with subsequent degenerative changes occurs under the exposure to IL17A. Thus, it has been found that the concentration of pro-inflammatory cytokines is significantly decreased in patients post total knee replacement [10–13].

Collagen, ensuring the connective tissue strength, elasticity, regulation, and regeneration, is the main structural component of extracellular matrix. Collagen type II is a component of cartilage tissue, being the main component of the alpha chain; it is encoded by the *COL2A1* gene [14, 15]. The *COL2A1* expression tissue-specific nature is a fundamental factor in determining the clinical features of associated diseases, divided into two groups depending on the affected tissue type. The first group includes developmental disorders of the musculoskeletal system (for example, dwarfism, kyphoscoliosis, limb shortening, joint abnormalities, hard palate malformations) and its functional competence in adulthood (for example, osteoarthritis affecting joints of various localizations). The second group includes extraskeletal abnormalities (hearing loss, eye disorder, such as myopia, retinal detachment, etc.) [16, 17].

Apoptosis, oxidative stress, age, nutrition, and hereditary factors are elements of the meniscus tissue degeneration process [18]. Apoptosis is triggered by activation of the CD95 receptor located on the cell membrane that is a member of the tumor necrosis factor α (TNF α) group [19]. The CD95 receptor triggering results in the emergence of a multi-protein complex, the interaction of which with the adapter molecules results in not only cell death, but also cell proliferation. Apoptosis most often occurs via the mitochondrial pathway, in which mitochondrial contents enter the cytoplasm due to activation of the p53 protein, activation of enzymes, DNA fragmentation, production of proapoptotic bodies and subsequent cell phagocytosis [20].

Nonsteroidal anti-inflammatory drugs (NSAIDs) are conventionally used for treatment of chondropathy of various origins, including osteoarthritis affecting joints. However, platelet-rich plasma (PRP) has become increasingly widely used in recent years. Various studies have shown that PRP can reduce inflammation and chondrocyte degeneration [21–24]. Photoactivated PRP enhances bioactivity and regeneration capacity of platelets through active release of growth factors contained in alpha granules, specifically the transforming growth factor β1 (TGF-β1), fibroblast growth factor, and platelet-derived growth factor [25]. The effectiveness of the treatment method used was demonstrated in large cohorts of patients, along with NSAIDs and glucocorticoids, but the mechanism underlying alteration of the secretory, phenotypic, and matrix profiles of chondrocytes in the meniscus tissue with degenerative alterations is poorly understood, it is of great interest in terms of determining biological targets when using PRP.

The study aimed to assess the effects of standard and photoactivated PRP on pro-inflammatory cytokine (IL6, IL17A) concentration, collagen type II (*COL2A1*) gene expression, and the CD95 apoptosis and meniscus degeneration marker in human meniscus fibrochondrocytes in the IL1β-induced inflammation *in vitro*.

METHODS

Chondrocytes isolated from the patients' knee joint menisci were used for the study; fragments of menisci were collected by arthroscopic resection during reconstruction of the anterior cruciate ligament. Experiments were conducted at the St. Luke Lugansk State Medical University.

The meniscus cartilage tissue samples were collected from 12 somatically healthy patients aged 18–35 years. Exclusion criteria: patients having systemic inflammatory disorders of immune and infectious origin; septic arthritis; treatment with intra-articular glucocorticoid injections throughout a month before the intervention. Inclusion criteria: degeneration of the knee meniscus verified based on the knee magnetic resonance imaging data and confirmed during arthroscopy; possibility of collecting sufficient quantities of tissue samples (4–8 mm^3 in total) to be later used in the experiment.

The collected meniscus tissue samples of all 12 donors were washed in phosphate buffered saline supplemented with penicillin (100 U/mL) and streptomycin (100 μg/mL), then crushed to 1–2 mm^3, and further treated with the 0.2% collagenase type II enzyme (Thermo Fisher Scientific, USA; catalog number 17101015, specific activity ≥ 125 U/mg (Mandl

units)). This enzyme was selected due to optimal ratio of the associated proteases, clostripain, and lipases essential for the hydrolysis of rigid collagen type II fibers. Cartilage disaggregation was conducted throughout 12 h at a temperature of 37 °C in the 5% CO_2 atmosphere with constant rocking. The resulting cell suspension was filtered through the nylon filter with the pore diameter of 70 μm and then centrifuged at 1500 rpm for 5 min. The isolated chondrocytes were cultured in the DMEM/F12 medium (Dulbecco's Modified Eagle Medium/Nutrient Mixture F-12) supplemented with the 10% fetal bovine serum and 1% penicillin and streptomycin solution at 37 °C, 5% CO_2. Cells from 2–3 passages were used for the experiment. Meniscus tissue samples from each donor were divided into four groups [26]: the first group remained unexposed, in all other samples degenerative damage was modeled by adding IL1β, standard PRP was added to cells of the third group, photoactivated PRP was added to cells of the fourth one.

Degenerative changes in the cells were induced by exposing the conjugated chondrocyte cultures (80–90%) to recombinant human IL1β (R&D Systems (Bio-Techne, USA; catalog number: 201-LB-005 per 5 μg) at a concentration of 10 ng/mL throughout 48 h. Such experimental approach was selected based on the earlier validated models of ostheoarthrosis and degenerative damage to meniscus tissue showing the IL1β-mediated activation of catabolic signaling pathways, degradation of the extracellular matrix, production of pro-inflammatory cytokines, and activation of apoptosis [27].

PRP was produced from the peripheral venous blood of the meniscus tissue donors after the admission and before the drug and surgical treatment in order to minimize the effects of medications used for anesthesia and further treatment. To strictly control the method reproducibility, avoid the cell composition contamination, and ensure dosage standardization, the Ycellbio test tubes (Ycellbio Medical Co., Ltd., Korea) and the two-step centrifugation protocol were used. Whole blood was collected straight in the test tubes containing 3.8% sodium citrate solution as an anticoagulant in a standard ratio. Sodium citrate was used strictly as an inhibitor of premature platelet activation during blood sampling and fractionation. The platelet concentrate isolation was performed using a specialized PLC-02 laboratory centrifuge (Ycellbio Medical Co., Ltd., Korea) equipped with the 45° fixed angle rotor with the maximum radius of rotation R_{max} = 13.5 cm. The first centrifugation was carried out at 1500 rpm (relative centrifugal force about 300 × g) for 10 min; after a few seconds, a second centrifugation was performed at 3500 rpm (relative centrifugal force about 1650× g) for 10 min. The resulting PRP produced in accordance with the manufacturer's instructions contained 1.0–1.2 × 10^6 platelets/μL, which corresponded to the 4–5-fold increase in platelet concentration compared to the baseline peripheral blood level. According to PAW (Platelet, Activation, White blood cells) classification: class P3-A (high platelet concentration, no previous exogenous activation, leukocyte-erythrocyte fraction) [28].

Photoactivation of experimental PRP samples without cartilage cells was performed by exposure to red light using a LED photoactivation system (Juventix LED Activator, USA) with the following settings: wavelength — 650 ± 10 nm, power density — 80 mW/cm^2, radiation spectrum full width at half maximum (FWHM) — 20 nm, beam divergence angle — 120°, exposure time — 7 min, distance from the light source — 10 cm, ambient temperature — 22–24 °C. The output power density (80 mW/cm^2) stability was ensured by a precision current power supply with the integrated power feedback, certified by the equipment manufacturer. Such parameters were selected to ensure the release of growth factors from alpha-granules of platelets due to more intense energy effect. Such PRP activation parameters were also selected considering the plasma optical density (possibility of light absorption by proteins). Immediately after photoactivation PRP added to the culture medium containing chondrocytes at the final concentration of 10% [29].

Biological samples obtained from each donor were evenly distributed across all experimental groups. Samples from each donor (n = 12 biological units (donors)) were coded with numbers, and laboratory tests were carried out in a blind manner. Cells from each donor were divided into four experimental groups, for each of which three technical replicates were performed: group 1 (control) — intact chondrocytes, no experimental exposure to interleukin; group 2 — chondrocytes exposed to IL1β supplemented with saline (0.9% sodium chloride solution); group 3 — cells altered under exposure to IL1β added PRP without photoactivation; group 4 — cells altered under exposure to IL1β added photoactivated PRP only. Equivalent volumes of saline (0.9% sodium chloride solution) and PRP were added. IL6, IL17A, CD95, *COL2A1* levels were assessed 48 h after the start of cell incubation with the addition of normal and photoactivated PRP.

The IL6, IL17A concentrations were determined using the R&D Systems kits (by Bio-Techne), series Quantikine ELISA (USA), in accordance with the manufacturer's protocol. The CD95 apoptosis marker was assessed using flow cytometry, the *COL2A1* expression was determined using the real-time polymerase chain reaction (RT-qPCR).

The *COL2A1* (collagen type II) expression levels were determined by the real-time quantitative polymerase chain reaction (RT-qPCR) in strict compliance with the MIQE international standard [30].

The total RNA extraction from the cartilage tissue samples was performed using the RNeasy Mini Kit (Qiagen, Germany) in accordance with the manufacturer's protocol. The extracted RNA concentration and purity were assessed by spectrophotometry using NanoDrop 2000 (Thermo Scientific, USA) based on the A260/A280 optical density ratio (within the range of 1.8–2.0). The RNA integrity was confirmed by the 1% agarose gel electrophoresis. The complementary DNA (cDNA) was synthesized from 1 μg of the total RNA using the RevertAid RT Reverse Transcription Kit (Thermo Scientific, USA) and the mixture of oligo (dT) and random primers.

To avoid errors associated with the use of only one unvalidated reference, the data were normalized to the geometric mean of two stable human genes: GAPDH (glyceraldehyde-3-phosphate dehydrogenase) and ACTB (β-actin). Human-specific oligonucleotide primers (NCBI Primer-BLAST) were selected at the boundaries of exon-exon junctions (intron-spanning) to avoid amplification of the genomic DNA. Amplification was accomplished in the CFX96 Touch system (Bio-Rad, USA) with the SYBR Green intercalating dye using the PowerUp SYBR Green Master Mix (Applied Biosystems, USA). The protocol included denaturation (95 °C, 2 min) and 40 cycles: denaturation (95 °C, 15 c), annealing/elongation (60 °C, 30 c). To verify product specificity after each launch, melting curves were analyzed with the range of 65–95 °C; in all reactions, a single melting peak without primer dimers was recorded. Each biological sample was tested in technological triplicates with the mandatory use of controls with no template (NTC) and no reverse transcriptase (NRT).

The amplification efficiency (E) was determined based on calibration curves of 5-fold serial dilutions of the cDNA pool. The straight line slope was between –3.31 and –3.34 (R_2 > 0.99), which showed high and comparable efficacy of reactions:

(E = 99.1%) for *COL2A1*, (E = 99.6%) for GAPDH, and (E = 98.9%) for ACTB. The *COL2A1* mRNA relative expression was calculated using the comparative 2-ΔΔ *Ct* method [31]. The Δ*Ct* value was determined as the difference between the threshold cycle of the target gene and the geometric mean of threshold cycles of reference genes (*CtCOL2A1* — geometric mean *Ct*ref). The final value of the fold change of expression was expressed relative to the control group (intact/healthy untreated cells).

Determination of the CD95 membrane receptor expression by flow cytometry

The CD95-positive cell counts and the receptor expression density on the membrane were assessed using a monoclonal mouse antibody against human CD95 (Mouse Anti-Human CD95, BioLegend, USA). The phycoerythrin (PE) fluorochrome was used for conjugation of antibodies (BioLegend, Inc., USA).

The chondrocyte suspension in the amount of 1×10^6 cells per test was precipitated by centrifugation at 300× g for 5 min. The cell sediment was resuspended in 100 µL of phosphate-buffered saline (PBS) containing 0.5% bovine serum albumin (BSA) and 2 mM EDTA (cytometry buffer). In order to minimize nonspecific binding via Fc receptors the samples were pre-incubated with the reagent for Fc receptor blockage (Human TruStain FcX (BioLegend), USA), 10 min at +4 °C. The Anti-CD95 monoclonal antibody was added (BioLegend, Inc., USA), 5 µL per test, and incubation was performed for 30 min in a dark place at a temperature of +4 °C. After the end of incubation the cells were twice washed with 1 mL of excess cold cytometry buffer by centrifugation (300× g, 5 min). The resulting sediment was resuspended in 300 µL of buffer. A vital dye, propidium iodide (PI) (Sigma-Aldrich (Merck), USA), at a concentration of 1 µg/mL was added to samples 5 min before the analysis in order to avoid artifacts.

Gating was performed in the BD FACSCanto II flow cytometer (BD Biosciences, USA), it involved recording of at least 50,000 target events for each sample. Data analysis was conducted using the FlowJo software (FlowJo, LLC (subsidiary of Becton, Dickinson and Company/BD Biosciences), USA). The live cell gating was performed by constructing the vital dye PI/7-AAD (Sigma-Aldrich, USA; BD Biosciences, USA) fluorescence distribution histogram. In further analyses, only the negative fraction dye was used ($PI^-/7\text{-}AAD^-$) to completely exclude dead cells from the CD95 expression analysis. Final gating was performed based on the fluorescence histogram in the PE detection channel through determination of the boundary (gate) separating $CD95^-$and $CD95^+$events. The boundary positioning was carried out strictly according to the upper fluorescence boundary of the isotype/FMO control (no more than 0.1–0.5% false positives were allows in the control). Quantity was assessed as a percentage of CD95-positive cells and the mean fluorescence intensity (MFI) reflecting the density of Fas receptors on the cell.

Data analysis was conducted in GraphPad Prism 9.4.1 (GraphPad Software, LLC (USA) and G*Power 3.1.9.7 (Heinrich Heine University Düsseldorf, Germany). A priori power calculation for the rm-ANOVA model (intragroup factor, four groups, $\alpha = 0.05$, power $1\text{-}\beta = 0.80$, expected large effect size f = 0.45 based on pilot data) defined the minimum sample size of n = 10. A total of 12 individual chondrocyte donors were included in the study. The distribution was tested for normality using the Shapiro–Wilk test and Q–Q plots [31], testing for homogeneity of variance was performed using the Levene's test [32], and that for sphericity was performed using the Mauchly's sphericity test. The rm-ANOVA (with the Greenhouse–Geisser correction for violation of sphericity) with the specified F-statistics F (f_{effect}, df_{error}) was used for related groups. Considering the simultaneous analysis of four indicators (IL6, IL17A, CD95, COL2A1), the critical significance level for rm-ANOVA was Bonferroni adjusted to $p_{crit} = 0.0125$). The pairwise post-hoc comparison was performed using the Tukey's test (p <0.05) based on the within-subject residual variance of the error (MS_{error}). The data are presented as mean ± SD and box-and-whisker plots with individual points. The 95% CI for the difference between means, partial eta-squared (η^2p) for the group factor, and the Cohen's d (d_z) for pairwise comparison were calculated.

RESULTS

Under the exposure of human meniscus chondrocytes to IL1β in vitro, the development of stable immune-inflammatory alterations, associated with the considerable increase in the levels of the studied pro-inflammatory cytokines, was reported within 48 h at the molecular level. The IL6 level increased 2.8-fold; $p < 0.05$; 95% CI for the difference between means: [48.2; 54.2]; $\eta^2 = 0.984$. Similar changes were reported for the IL17A concentration that increased 3-fold, $p < 0.05$; 95% CI for the difference between means: [26.8; 30.4]; $\eta^2 = 0.984$. In the cell cultures of donors included in group 2, the percentage of CD95-positive chondrocytes increased 4.2-fold, $p < 0.05$; 95% CI for the difference between means: [20.1; 23.3]; $\eta^2 = 0.980$), which suggests the fibrochondrocyte apoptosis initiation at the phenotype level. At the same time the expression of the main matrix protein COL2A1 was depressed 2.4-fold, $p < 0.05$; 95% CI for the difference between means: [–0.62; –0.54]; $\eta^2 = 0.954$, which may indicate the collagen synthesis suppression and its degradation under the exposure to IL1β (Table 1).

Adding standard PRP to the meniscus cell samples resulted in partial mitigation of induced inflammatory and degenerative processes in all the studied cultures. This clearly manifested itself in the 1.4-fold decrease in the IL6 concentration; $p < 0.05$; 95% CI for the difference between means: [–27.1; –21.9]; $\eta^2 = 0.911$, 1.5 decrease in the IL17A concentration; $p < 0.05$; 95% CI for the difference between means: [–15.4; –11.4]; $\eta^2 = 0.879$. At the cell phenotype level, the percentage of CD95-positive cells decreased 1.66-fold; $p < 0.05$; 95% CI for the difference between means: [–12.8; –9.8]; $\eta^2 = 0.919$. The *COL2A1* gene expression increased 1.7-fold, $p < 0.05$; 95% CI for the difference between means: [0.24; 0.34]; $\eta^2 = 0.896$ (Table 2).

After adding photoactivated PRP, a significant regression of inflammatory chondrocyte alteration was reported in all the studied groups. The IL6 levels decreased 1.4-fold; $p < 0.05$; 95% CI for the difference between means: [–19.1; –14.7]; $\eta^2 = 0.970$ compared to the values obtained after adding standard PRP. The IL17A concentration decreased 1.6-fold; $p < 0.05$; 95% CI for the difference between means: [–12.1; –9.5]; $\eta^2 = 0.972$. At the phenotype level, the 1.8-fold decrease in the percentage of CD95-positive cells was observed after adding photoactivated PRP; $p < 0.05$; 95% CI for the difference between means: [–8.4; –7.2]; $\eta^2 = 0.975$ compared to the groups of cells treated with standard PRP. The *COL2A1* gene expression increased 1.3-fold, $p < 0.05$; 95% CI for the difference between means: [0.18; 0.28]; $\eta^2 = 0.931$, which was almost compared with the values of the intact group (Table 3).

The dynamic changes in the studied indicators for all groups of *in vitro* cultures of the human meniscus cartilage are presented in Fig.

Table 1. Effects of interleukin-1β on the secretory, phenotypic and matrix profiled of human meniscus chondrocytes *in vitro* after the 48-h incubation (M ± SD [95% CI], *n* = 12)

Indicator	Control	*p*	IL1β + 0,9% NaCl	*p*
IL6 (pg/mL)	28.4 ± 2.1 [27.1; 29.7]	0.01	79.6 ± 4.3* [76.9; 82.3]	0.04
IL17A (pg/mL)	14.2 ± 1.0 [13.6; 14.8]	0.05	42.8 ± 2.5* [41.2; 44.4]	0.05
CD95 (%)	6.8 ± 0.7 [6.4; 7.2]	0.04	28.5 ± 2.2* [27.1; 29.9]	0.05
COL2A1 (2-ΔΔ *Ct*)	1.00 ± 0.08 [0.95; 1.05]	0.001	0.42 ± 0.05* [0.39; 0.45]	0.001

Note: * — $p < 0.05$ compared to control.

The IL6 concentration in group 2 increased by 180.3% (2.8-folda), IL17A concentration increased by 201.4% (3-fold), CD95 level increased by 319.1% (4.2-fold), and *COL2A1* level decreased by 58.0% (2.4-fold) compared to the control group (Fig.). The use of standard PRP resulted in the IL6 decrease by 30.8%, IL17A decrease by 31.3%, CD95 decrease by 39.6%; *COL2A1* increased by 69.0% compared to group 2. The use of photoactivated PRP resulted in the decrease in the levels of pro-inflammatory cytokines: IL6 by 52.01% (2.08-fold), IL17A by 5654% (2.30-fold), CD95 apoptosis marker by 67.02% (3.03-fold); *COL2A1* increased by 123.81% (2.24-fold) compared to group 2. When compared to the indicators of group 3, the effect of photoactivated PRP was superior to that of standard PRP: for IL6 — by 30.67% (1.44-fold), for IL17A — by 36.73% (1.58-fold), for CD95 — by 45.35% (1.83-fold); the *COL2A1* growth by 32.39% (1.32-fold) was reported, confirmed by the paired post-hoc Tukey's test.

DISCUSSION

The meniscus tissue degeneration is accompanied by low-grade inflammation due to the increase in the levels of pro-inflammatory cytokines, as well as by the cartilage tissue volume reduction [1, 5, 7]. In our study, the exposure to IL1β resulted in triggering the immune inflammation and the meniscus tissue degeneration *in vitro* as early, as 48 h after incubation. This is supported by the considerable increase in IL6 and IL17A levels compared to the control group, the increase in apoptosis marker levels, and the decrease in the *COL2A1* gene expression. This fact suggests that the more prolonged exposure to IL1β may result in more pronounced alterations, being one of the key cytokines of the degenerative damage to the meniscus tissue [8].

The *COL2A1* was selected as one of the molecular indicators of the meniscus fibrocartilaginous tissue due to its high pathogenetic significance for modeling osteoarthritis. The meniscus tissue is heterogeneous due to predominance of collagen type I ensuring elasticity in the vascular zone; the structure of the avascular zone that was collected for the study was close to that of the hyaline cartilage due to chondrocyte-like cells and the expression of collagen type II [33]. In the osteoarthritis- and obesity-associated inflammation, a phenotypic shift occurs in the meniscus cells, resulting in apoptosis and the decreased collagen type II synthesis (COL2A1). This gene is a marker of the meniscus avascular zone extracellular matrix degeneration and loss of shock-

Table 2. Effects of platelet-rich plasma on the inflammatory, phenotypic, and matrix profiles of human meniscus chondrocytes *in vitro* in the context of interleukin-1β-induced inflammation (M ± SD [95% CI], *n* = 12).

Indicator	IL1β + 0,9% NaCl	*p*	IL1β + PRP	*p*
IL6 (pg/mL)	79.6 ± 4.3 [76.9; 82.3]	0.04	55.1 ± 3.4# [52.9; 57.3]	0.001
IL17A (pg/mL)	42.8 ± 2.5 [41.2; 44.4]	0.05	29.4 ± 2.1# [28.1; 30.7]	0.05
CD95 (%)	28.5 ± 2.2 [27.1; 29.9]	0.05	17.2 ± 1.5# [16.2; 18.2]	0.01
COL2A1 (2-ΔΔ *Ct*)	0.42 ± 0.05 [0.39; 0.45]	0.001	0.71 ± 0.06# [0.67; 0.75]	0.04

Note: # — $p < 0.05$ compared to the group of IL1β.

Table 3. Comparative analysis of the effects of standard and photoactivated platelet-rich plasma on the inflammatory, phenotypic, and matrix profiles of human meniscus chondrocytes *in vitro* in the context of interleukin-1β-induced inflammation (M ± SD [95% CI], *n* = 12).

Indicator	IL1β + PRP	*p*	IL1β + photoactivated PRP	*p*
IL6 (pg/mL)	55.1 ± 3.4 [52.9; 57.3]	0.001	38.2 ± 2.6† [36.5; 39.9]	0.01
IL17A (pg/mL)	29.4 ± 2.1 [28.1; 30.7]	0.05	18.6 ± 1.7† [17.5; 19.7]	0.001
CD95 (%)	17.2 ± 1.5 [16.2; 18.2]	0.01	9.4 ± 0.8† [8.9; 9.9]	0.003
COL2A1 (2-ΔΔ *Ct*)	0.71 ± 0.06 [0.67; 0.75]	0.04	0.94 ± 0.07† [0.90; 0.98]	0.04

Note: † — $p < 0.05$ compared to the group of standard PRP.

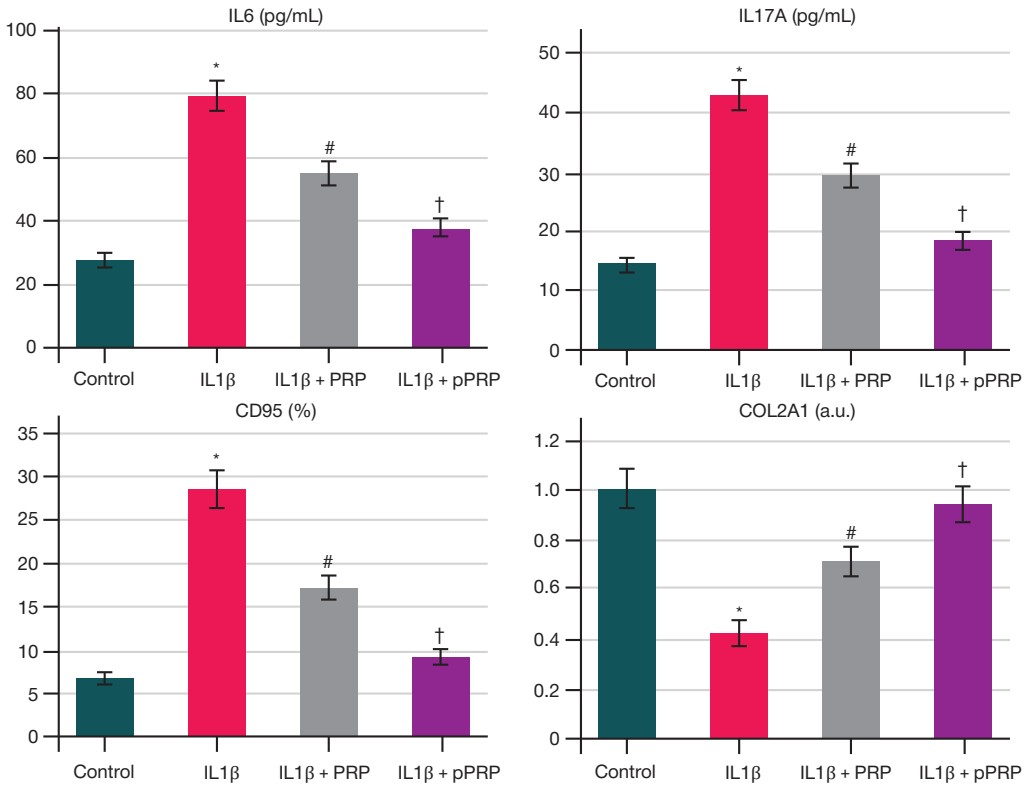

Fig. 1. Inflammatory (IL6, IL17A), phenotypic (CD95), and matrix (COL2A1) profiles of human meniscus chondrocytes *in vitro* I the IL1β-induced inflammation adjusted with standard and photoactivated PRP. Control — intact control group not exposed to IL1β; IL1β + 0,9% NaCl — group 2, IL1β + PRP — group 3; IL1β + p PRP — group 4. Each individual point on the graph corresponds to the average value of technical replicates for one biological donor out of 12. # — $p < 0.05$ compared to the "IL1β" group; † — $p < 0.05$ compared to the "IL1β + PRP" group (post-hoc Tukey's test for repeated measurements)

absorbing properties, up to the emergence of perforations [34]. Assessment of this indicator makes it possible to verify the therapy capability of preserving the chondrocyte-like phenotype of the meniscus cells and blocking the catabolic cascade, which cannot be assessed by analyzing distinct fibrous tissue substitution markers only (of collagen type I) [35].

Adjustment with platelet-rich plasma that can reduce the degenerative alteration manifestations in chondrocytes leads to the reduction of inflammation, which is similar to the effects of nonsteroidal anti-inflammatory drugs or glucocorticoids [2, 21–24]. Furthermore, PRP contains no additional chemical components. It contains only platelets that, in addition to their regenerative properties, can reduce manifestations of inflammation. The decrease in the IL6, IL17A, and CD95 marker concentrations was determined, along with the increase in the COL2A1 expression due to the PRP biological activity. Some in vitro and ex vivo studies suggest that PRP can cause chondrocyte proliferation. This process can come at the expense of mature cells, which, under similar conditions, exhibit the properties of fibroblasts, reducing the *COL2A1* expression, and synthesize the fibrous collagen type I (*COL2A1*) [36]; this was not confirmed in our study.

As determined in our experiment, the use of photoactivated plasms leads to further enhancement of the platelet biological activity and regenerative capacity. This can be due to the active release of the platelet-derived growth factors deposited in alpha granules and the inflammatory signaling pathway modulation. The key role in the fibrocartilaginous tissue regeneration and reduction of damage is played by the transforming growth factor β-1 (TGF-β1), fibroblast growth factor (bFGF/FGF2), and platelet-derived growth factor (PDGF) [24, 25]. The reported molecular genetic and cellular effects were especially significant in group 4: the IL6, IL17A, and CD95 levels decreased and the *COL2A1* gene expression increased almost to the values of intact chondrocytes in group 1. The pro-inflammatory cytokine levels decreased due to inhibition of the key transcription factor NF-κB (nuclear factor kappa B). Phosphorylation and degradation of the IκB inhibitory protein are blocked under the exposure to PRP, which later leads to the knockout of the genes encoding pro-inflammatory cytokines. Photoactivation leads to the enhancement of such effect through activation of the mitochondrial cytochrome C oxidase activation, adenosine triphosphoric acid (ATP) stimulation, and the short-term release of reactive oxygen species activating endogenous pro-inflammatory factors. The phosphorylation cascade activation leads to inhibition of proapoptotic proteins of the Bcl-2 family (Bax and Bad), FoxO transcription factor blockage, resulting in the CD95 receptor deactivation and further triggering of effector caspases [37].

The *COL2A1* gene expression increase following adding photoactivated PRP results from activation of the Smad2/3 signaling pathway under the exposure to TGF-β1 binding to the TGFBR1/TGFBR2 receptors. As a result, the Smad2 and Smad3 protein phosphorylation occurs. The resulting complex translocates to the nuclear region and binds to the SOX9 gene promoter responsible for chondrogenesis. When activated, the gene ensures triggering of the *COL2A1* mRNA expression cascade, resulting in the increased synthesis of collagen type II and the increased density of the meniscus extracellular matrix [38]. The use od standard PRP has less potential for *COL2A1* compared to the photoactivated form, since the degranulation kinetics are lower. Sharp and excessive proliferative stimulation of chondrocytes with standard PRP can cause their transient differentiation, leading to the suppression of the synthesis of key structural markers [39]. When the irradiation protocol is violated, photoactivated plasma may have restructured degranulation kinetics, providing a prolonged release of growth factors (PDGF, bFGF). The excess of the latter leads to continuous division of

chondrocytes, causing the shutdown of anabolic synthesis of the cellular matrix *COL2A1* and ACAN [25].

The experimental data obtained suggest the possibility of using platelet-rich plasma by the standard method and with photoactivation for the cartilage tissue regeneration, as well as using it for reconstructive surgery of the meniscus and chondroplasty.

Limitations of the study

The exceptionally high effect size (η^2 = 0.879–0.984) and low inter-donor variability (CV ≈ 5–8%) reported for human material result from the strict biological standardization (use of early passage cells, synchronization of the cell cycle) and mathematical specificity of the rm-ANOVA model. Such a design isolates the donors' individual variability from the error variance, thereby naturally inflating the share of variance (η^2p) explained by the group factor and possibly limiting the direct extrapolation of the data *in vivo*.

CONCLUSIONS

During the study it has been found that the exposure of the culture of human meniscus tissue chondrocytes to IL1β *in vitro* leads to the increase in the concentrations of pro-inflammatory cytokines IL6, IL17 and the $CD95^+$ cell apoptosis marker, as well as to the decrease in the *COL2A1* gene expression in the culture. Such alterations demonstrate an immune inflammatory pattern with triggering the chondrocyte apoptosis and the extracellular matrix degradation in the cartilage under the exposure to IL1β. The use of PRP possessing biological activity and having a regeneration potential due to high platelet counts can reduce the severity of inflammation and apoptosis in the cartilage tissue, it positively affects regeneration and the collagen type II synthesis, i.e. effectively affects on the secretory (IL6, IL17A), matrix (*COL2A1*), and phenotypic (*CD95*) profiles of human meniscus fibrochondrocytes in the IL1β-induced inflammation *in vitro*. The study has shown that photoactivated PRP can have a more pronounced biological effect on all the studied parameters due to more active release of growth factors by platelets accompanied by normalization of the secretory, phenotypic, and matrix profiles. Further exploration of the effects of standard and photoactivated PRP in clinical practice with the development of optimal terms and frequency of intra-articular administration will make it possible to assess the chondrocyte regeneration mechanism when selecting a cell-based therapy method in patients with the meniscus cartilage tissue degeneration, including osteoarthritis.

References

1. Gladkova EV, Ivanov AN. Vzaimosvyaz' strukturnyh narushenij sustavnogo gialinovogo hryashcha i parametrov sistemnyh proyavlenij vospalitel'noj reakcii v patogeneze rannih stadij pervichnogo osteoartroza. Saratovskij nauchno-medicinskij zhurnal. 2018; 14 (3): 518–23. Dostupno po ssylke: https://cyberleninka.ru/article/n/vzaimosvyaz-strukturnyh-narusheniy-sustavnogo-gialinovogo-hryascha-i-parametrov-sistemnyh-proyavleniy-vospalitelnoy-reaktsii-v (data obrashcheniya: 27.06.2026). Russian.
2. Ivanov AS, Tananakina TP, Kashchenko SA, Pogorelova IA. Expression of microRNA miR146a in the blood plasma of rats with obesity and knee arthrosis after administration of dexamethasone. Bulletin of RSMU. 2025; 6: 209–15. DOI: 10.24075/brsmu.2025.056.
3. Plekhova NG, Kabalyk MA, Prosekova EV, Shumatov VB. Provospalitel'nye citokiny, hemokin CXSL17 i belki teplovogo shoka pri osteoartrite kolennogo sustava. Rossijskij immunologicheskij zhurnal. 2025; 28 (1): 129–34. DOI: 10.46235/1028-7221-16975-PCC. Russian.
4. Chow YY, Chin KY. The Role of Inflammation in the Pathogenesis of Osteoarthritis. Mediators Inflamm. 2020; 2020: 8293921. DOI: 10.1155/2020/8293921.
5. McGregor NE, Murat M, Elango J, Poulton IJ, Walker EC, et al. IL6 exhibits both cis- and trans-signaling in osteocytes and osteoblasts, but only trans-signaling promotes bone formation and osteoclastogenesis. J Biol Chem. 2019; 294 (19): 7850–63. DOI: 10.1074/jbc.RA119.008074.
6. Vadalà G, Di Giacomo G, Ambrosio L, Cannata F, Cicione C, Papalia R, Denaro V. Irisin Recovers Osteoarthritic Chondrocytes In Vitro. Cells. 2020; 9 (6): 1478. DOI: 10.3390/cells9061478.
7. Li L, Li Z, Li Y, Hu X, Zhang Y, et al. Profiling of inflammatory mediators in the synovial fluid related to pain in knee osteoarthritis. BMC Musculoskelet Disord. 2020; 21 (1): 99. DOI: 10.1186/s12891-020-3120-0.
8. Fedulichev NP. Provospalitel'nye citokiny v patogeneze osteoartrita. Universitetskaya klinika. 2024; 4 (53): 70–81. Dostupno po ssylke: https://cyberleninka.ru/article/n/provospalitelnye-tsitokiny-v-patogeneze-osteoartrita (data obrashcheniya: 27.06.2026). Russian.
9. Jaime P, García-Guerrero N, Estella R, Pardo J, GarcíaÁlvarez F, et al. CD56+/CD16- Natural Killer cells expressing the inflammatory protease granzyme are enriched in synovial fluid from patients with osteoarthritis. Osteoarthritis Cartilage. 2017; 25 (10): 1708–18. DOI: 10.1016/j.joca.2017.06.007.
10. Mimpen JY, Carr AJ, Dakin SG, Snelling SJ. Inhibition of interleukin-17-induced effects in osteoarthritis — An in vitro study. Osteoarthritis Cartilage. 2018; 26: S118. DOI: 10.1016/j.joca.2018.02.258.
11. Babaei M, Javadian Y, Narimani H, Ranaei M, Heidari B, et al. Correlation between systemic markers of inflammation and local synovitis in knee osteoarthritis. Caspian J Intern Med. 2019; 10 (4): 383–7. DOI: 10.22088/ cjim.10.4.383.
12. Snelling SJ, Bas S, Puskas GJ, Dakin SG, Suva D, et al. Presence of IL17 in synovial fluid identifies a potential inflammatory osteoarthritic phenotype. PLoS One. 2017; 12 (4): e0175109. DOI: 10.1371/journal.pone.0175109.
13. Lee YH, Song GG. Association between IL17 gene polymorphisms and circulating IL17 levels in osteoarthritis: a meta-analysis. Z Rheumatol. 2020; 79 (5): 482–90. DOI: 10.1007/s00393-019-00720-2.
14. Dydykina IS, Kovalenko PS, Kovalenko AA, Aboleshina AV. Znachenie nedenaturirovannogo kollagena dlya normalizacii funkcii hryashchevoj tkani sustavov. Medicinskij sovet. 2022; 16 (14): 145–53. DOI: 10.21518/2079- 701X-2022-16-14-145-153. Russian.
15. Zhang B, Zhang Y, Wu N, Li J, Liu H, Wang J. Integrated analysis of COL2A1 variant data and classification of type II collagenopathies. Clin Genet. 2020; 97: 383–95. DOI: 10.1111/cge.13680.
16. Mortier GR, Cohn DH, Cormier-Daire V, Hall C, Krakow D, Mundlos S, et al. Nosology and classification of genetic skeletal disorders: 2019 revision. Am J Med Genet A. 2019; 179 (12): 2393–419. DOI: 10.1002/ajmg.a.61366.
17. Viakhireva I, Bychkov I, Markova T, Shatokhina O, Karandasheva K, Udalova V, Bekhtereva Y, Ryzhkova O, Skoblov M. The molecular complexity of COL2A1 splicing variants and their significance in phenotype severity. Bone. 2024; 181: 117013. DOI: 10.1016/j.bone.2024.117013.
18. Huan Yu, Sai Yao, Chengchong Zhou, Fangda Fu, Huan Luo, Weibin Du, et al. Morroniside attenuates apoptosis and pyroptosis of chondrocytes and ameliorates osteoarthritic development by inhibiting NF-κB signaling. Journal of Ethnopharmacology. 2021; 266: 113447. DOI: 10.1016/j.jep.2020.113447.
19. Hussain A, Tarahomi T, Singh L, Bollampally M, Heydari-Kamjani M, Kesselman MM. Cardiovascular Risk Associated with TNF Alpha Inhibitor Use in Patients with Rheumatoid Arthritis. Cureus. 2021;

13 (9): e17938. DOI: 10.7759/cureus.17938.
20. Abramova TYa, Blinova EA, Pashkina EA, Grishina LV, Ilina NA, Chumasova O. A., i dr. Issledovanie effektornyh molekul avtonomnogo i neavtonomnogo vliyaniya apoptoza T-limfocitov v usloviyah «kletochnogo sosedstva» v kul'ture u zdorovyh lyudej i pacientov s RA. Medicinskaya immunologiya. 2022; 24 (6): 1119–38. DOI: 10.15789/1563-0625-SOE-2527. Russian.
21. Bagmut IYu, Ivanov OS, Sheremet MI, Smirnov SM, Kolisnyk IL, Ivanova JV, et al. Isolation of megakaryocytes using magnetic cell separation and adverse effects induced by diclofenac toxicity in an experiment. J Med Life. 2022; 15 (1): 65–70. DOI: 10.25122/jml-2020-0129.
22. Ivanov O, Haidash O, Voloshin V, Kondratov S, Smirnov A. Influence of the acting substance sodium diclofenac on bone marrow cells. Georgian Medical News. 2020; 306: 137–42. PMID: 33130661.
23. Ivanova YuV, Gramatiuk SM, Kryvoruchko IA, Prasol VO, Pulyaeva IS, Miasoiedov KV, et al. The Effect of pulsed photobiomodulation on proliferation and migration of human mesenchymal stem cells in vitro. Clinical and preventive medicine. 2024; (5): 87–92. DOI: 10.31612/2616-4868.5.2024.11.
24. Medvedev VL, Opolskij AM, Kogan MI. Perspektivy razvitiya regenerativnyh tekhnologij. Sovremennye znaniya ob autoplazme, obogashchennoi trombocitami i vozmozhnosti ee primeneniya v lechenii urologicheskih zabolevanii. Kubanskij nauchnyj medicinskij vestnik. 2018; 25 (3): 155–61. DOI: 10.25207/1608-6228-2018-25-3-155-161.
25. Irmak G, Gümüşderelioğlu M. Photo-activated platelet-rich plasma (PRP)-based patient-specific bio-ink for cartilage tissue engineering. Biomed Mater. 2020; 15 (6): 065010. DOI: 10.1088/1748-605X/ab9e46.
26. Gramatiuk S, Kryvoruchko I, Ivanova Y, Emily Hubbard, Maria Noebauer-Babenko, Karine Sargsyan. Artificial Intelligence-Based Quality Control of Cell Lines. Biopreserv Biobank. 2025; DOI: 10.1177/19475535251367317.
27. Li Y, Wang F, Ji B, Amati A, Cao L. FHL2 deteriorates IL-1β induced inflammation, apoptosis, and extracellular matrix degradation in chondrocyte-like ATDC5 cells by mTOR and NF-κB pathways. BMC Musculoskelet Disord. 2025; 26 (1): 331. DOI: 10.1186/s12891-025-08536-9.
28. Collins T, Alexander D, Barkatali B. Platelet-rich plasma: a narrative review. EFORT Open Rev. 2021; 6 (4): 225–35. DOI: 10.1302/2058-5241.6.200017.
29. Mishra Kanchan, Desai Pooja, Khanna Manish, Malhotra Sayesha. Photoactivated platelet-rich plasma (PA-PRP): A safe and effective treatment for musculoskeletal disorders. IP International Journal of Orthopaedic Rheumatology. 2025; 11: 71–75. DOI: 10.18231/j.ijor.25218.1765359797.
30. Bustin SA, Ruijter JM, van den Hoff MJB, Kubista M, Pfaffl MW, Shipley GL, et al. MIQE 2.0: Revision of the Minimum Information for Publication of Quantitative Real-Time PCR Experiments Guidelines. Clin Chem. 2025; 71 (6): 634–51. DOI: 10.1093/clinchem/hvaf043.
31. Videla-Jiménez P, Ruz F, López-Martín M. Research on box plot knowledge in statistical education: a systematic review of the literature. Eur J Psychol Educ. 2025; 40: 141. DOI: 10.1007/s10212-025-01048-z.
32. Livak KJ, Schmittgen TD. Analysis of relative gene expression data using real-time quantitative PCR and the 2(-Delta Delta C(T)) Method. Methods. 2001; 25 (4): 402–8. DOI: 10.1006/meth.2001.1262.
33. Raut RD, Chakraborty AK, Neogi T, Michael Albro, Brian Snyder, Thomas P. Schaer, et al. A multi-tissue human knee single-cell atlas identifies that osteoarthritis reduces regenerative tissue stem cells while increasing inflammatory pain macrophages. Commun Biol. 2025; 8: 1146. DOI: 10.1038/s42003-025-08586-8.
34. Mocanu V, Timofte DV, Zară-Dănceanu C-M, Labusca L, Obesity. Metabolic Syndrome, and Osteoarthritis Require Integrative Understanding and Management. Biomedicines. 2024; 12: 1262. DOI: 10.3390/biomedicines12061262.
35. Galicia-Canales BE, del Rocío Aguilar-Gaytán M, Álvarez-Pérez MA, Jarquín-Yáñez K, et al. Effect of peniocerol on human meniscal fibrochondrocyte inflammation induced by IL-1β and TNF-α through the NF-κB signaling pathway. Cellular and Molecular Biology. 2026; 72 (3): 36–44. DOI: 10.14715/cmb/2025.72.3.5.
36. Rikkers M, Dijkstra K, Terhaard BF, Admiraal J, Levato R, Malda J, et al. Platelet-Rich Plasma Does Not Inhibit Inflammation or Promote Regeneration in Human Osteoarthritic Chondrocytes In Vitro Despite Increased Proliferation. Cartilage. 2021; 13 (2_suppl): 991S–1003S. DOI: 10.1177/1947603520961162.
37. Zhao H, Zhu W, Mao W, Shen C. Platelet-rich plasma inhibits Adriamycin-induced inflammation via blocking the NF-κB pathway in articular chondrocytes. Mol Med. 2021; 27 (1): 66. DOI: 10.1186/s10020-021-00314-2.
38. O'Donnell C, Migliore E, Grandi FC, et al. Platelet-Rich Plasma (PRP) From Older Males With Knee Osteoarthritis Depresses Chondrocyte Metabolism and Upregulates Inflammation. J Orthop Res. 2019; 37: 1760–70. DOI: 10.1002/jor.24322.
39. Li M, Jing C, Liu Q, Zhang Y, Li K. Platelet-rich plasma in cartilage repair: biological mechanisms and clinical perspectives. Front Sports Act Living. 2026; 8: 1785754. DOI: 10.3389/fspor.2026.1785754.

Литература

1. Гладкова Е. В., Иванов А. Н. Взаимосвязь структурных нарушений суставного гиалинового хряща и параметров системных проявлений воспалительной реакции в патогенезе ранних стадий первичного остеоартроза. Саратовский научно-медицинский журнал. 2018; 14 (3): 518–23. Доступно по ссылке: https://cyberleninka.ru/article/n/vzaimosvyaz-strukturnyh-narusheniy-sustavnogo-gialinovogo-hryascha-i-parametrov-sistemnyh-proyavleniy-vospalitelnoy-reaktsii-v (дата обращения: 27.06.2026).
2. Иванов А. С., Тананакина Т. П., Кащенко С. А., Погорелова И. А. Экспрессия микроРНК miR146a в плазме крови крыс с ожирением и артрозом коленного сустава на фоне введения дексаметазона. Вестник РГМУ. 2025; 6: 223–9. DOI: 10.24075/vrgmu.2025.056.
3. Плехова Н. Г., Кабалык М. А., Просекова Е. В., Шуматов В. Б. Провоспалительные цитокины, хемокин CXCL17 и белки теплового шока при остеоартрите коленного сустава. Российский иммунологический журнал. 2025; 28 (1): 129–34. DOI: 10.46235/1028-7221-16975-PCC.
4. Chow YY, Chin KY. The Role of Inflammation in the Pathogenesis of Osteoarthritis. Mediators Inflamm. 2020; 2020: 8293921. DOI: 10.1155/2020/8293921.
5. McGregor NE, Murat M, Elango J, Poulton IJ, Walker EC, et al. IL6 exhibits both cis- and trans-signaling in osteocytes and osteoblasts, but only trans-signaling promotes bone formation and osteoclastogenesis. J Biol Chem. 2019; 294 (19): 7850–63. DOI: 10.1074/jbc.RA119.008074.
6. Vadalà G, Di Giacomo G, Ambrosio L, Cannata F, Cicione C, Papalia R, Denaro V. Irisin Recovers Osteoarthritic Chondrocytes In Vitro. Cells. 2020; 9 (6): 1478. DOI: 10.3390/cells9061478.
7. Li L, Li Z, Li Y, Hu X, Zhang Y, et al. Profiling of inflammatory mediators in the synovial fluid related to pain in knee osteoarthritis. BMC Musculoskelet Disord. 2020; 21 (1): 99. DOI: 10.1186/s12891-020-3120-0.
8. Федуличев Н. П. Провоспалительные цитокины в патогенезе остеоартрита. Университетская клиника. 2024; 4 (53): 70–81. Доступно по ссылке: https://cyberleninka.ru/article/n/provospalitelnye-tsitokiny-v-patogeneze-osteoartrita (дата обращения: 27.06.2026).
9. Jaime P, García-Guerrero N, Estella R, Pardo J, GarcíaÁlvarez F, et al. CD56+/CD16- Natural Killer cells expressing the inflammatory protease granzyme are enriched in synovial fluid from patients with osteoarthritis. Osteoarthritis Cartilage. 2017; 25 (10): 1708–18. DOI: 10.1016/j.joca.2017.06.007.
10. Mimpen JY, Carr AJ, Dakin SG, Snelling SJ. Inhibition of interleukin-17-induced effects in osteoarthritis — An in vitro study. Osteoarthritis

Cartilage. 2018; 26: S118. DOI: 10.1016/j.joca.2018.02.258.
11. Babaei M, Javadian Y, Narimani H, Ranaei M, Heidari B, et al. Correlation between systemic markers of inflammation and local synovitis in knee osteoarthritis. Caspian J Intern Med. 2019; 10 (4): 383–7. DOI: 10.22088/ cjim.10.4.383.
12. Snelling SJ, Bas S, Puskas GJ, Dakin SG, Suva D, et al. Presence of IL17 in synovial fluid identifies a potential inflammatory osteoarthritic phenotype. PLoS One. 2017; 12 (4): e0175109. DOI: 10.1371/journal.pone.0175109.
13. Lee YH, Song GG. Association between IL17 gene polymorphisms and circulating IL17 levels in osteoarthritis: a meta-analysis. Z Rheumatol. 2020; 79 (5): 482–90. DOI: 10.1007/s00393-019-00720-2.
14. Дыдыкина И. С., Коваленко П. С., Коваленко А. А., Аболешина А. В. Значение неденатурированного коллагена для нормализации функции хрящевой ткани суставов. Медицинский совет. 2022; 16 (14): 145–53. DOI: 10.21518/2079- 701X-2022-16-14-145-153.
15. Zhang B, Zhang Y, Wu N, Li J, Liu H, Wang J. Integrated analysis of COL2A1 variant data and classification of type II collagenopathies. Clin Genet. 2020; 97: 383–95. DOI: 10.1111/cge.13680.
16. Mortier GR, Cohn DH, Cormier-Daire V, Hall C, Krakow D, Mundlos S, et al. Nosology and classification of genetic skeletal disorders: 2019 revision. Am J Med Genet A. 2019; 179 (12): 2393–419. DOI: 10.1002/ajmg.a.61366.
17. Viakhireva I, Bychkov I, Markova T, Shatokhina O, Karandasheva K, Udalova V, Bekhtereva Y, Ryzhkova O, Skoblov M. The molecular complexity of COL2A1 splicing variants and their significance in phenotype severity. Bone. 2024; 181: 117013. DOI: 10.1016/j.bone.2024.117013.
18. Huan Yu, Sai Yao, Chengchong Zhou, Fangda Fu, Huan Luo, Weibin Du, et al. Morroniside attenuates apoptosis and pyroptosis of chondrocytes and ameliorates osteoarthritic development by inhibiting NF-κB signaling. Journal of Ethnopharmacology. 2021; 266: 113447. DOI: 10.1016/j.jep.2020.113447.
19. Hussain A, Tarahomi T, Singh L, Bollampally M, Heydari-Kamjani M, Kesselman MM. Cardiovascular Risk Associated with TNF Alpha Inhibitor Use in Patients with Rheumatoid Arthritis. Cureus. 2021; 13 (9): e17938. DOI: 10.7759/cureus.17938.
20. Абрамова Т. Я., Блинова Е. А., Пашкина Е. А., Гришина Л. В., Ильина Н. А., Чумасова О. А., Сизиков А. Э., Козлов В. А. Исследование эффекторных молекул автономного и неавтономного влияния апоптоза Т-лимфоцитов в условиях «клеточного соседства» в культуре у здоровых людей и пациентов с РА. Медицинская иммунология. 2022; 24 (6): 1119–38. DOI: 10.15789/1563-0625-SOE-2527.
21. Bagmut IYu, Ivanov OS, Sheremet MI, Smirnov SM, Kolisnyk IL, Ivanova JV, et al. Isolation of megakaryocytes using magnetic cell separation and adverse effects induced by diclofenac toxicity in an experiment. J Med Life. 2022; 15 (1): 65–70. DOI: 10.25122/jml-2020-0129.
22. Ivanov O, Haidash O, Voloshin V, Kondratov S, Smirnov A. Influence of the acting substance sodium diclofenac on bone marrow cells. Georgian Medical News. 2020; 306: 137–42. PMID: 33130661.
23. Ivanova YuV, Gramatiuk SM, Kryvoruchko IA, Prasol VO, Pulyaeva IS, Miasoiedov KV, et al. The Effect of pulsed photobiomodulation on proliferation and migration of human mesenchymal stem cells in vitro. Clinical and preventive medicine. 2024; (5): 87–92. DOI: 10.31612/2616-4868.5.2024.11.
24. Медведев В. Л., Опольский А. М., Коган М. И. Перспективы развития регенеративных технологий. Современные знания об аутоплазме, обогащеннои тромбоцитами и возможности ее применения в лечении урологических заболеваний. Кубанский научный медицинский вестник. 2018; 25 (3): 155–61. DOI: 10.25207/1608-6228-2018-25-3-155-161.
25. Irmak G, Gümüşderelioğlu M. Photo-activated platelet-rich plasma (PRP)-based patient-specific bio-ink for cartilage tissue engineering. Biomed Mater. 2020; 15 (6): 065010. DOI: 10.1088/1748-605X/ab9e46.
26. Gramatiuk S, Kryvoruchko I, Ivanova Y, Emily Hubbard, Maria Noebauer-Babenko, Karine Sargsyan. Artificial Intelligence-Based Quality Control of Cell Lines. Biopreserv Biobank. 2025; DOI: 10.1177/19475535251367317.
27. Li Y, Wang F, Ji B, Amati A, Cao L. FHL2 deteriorates IL-1β induced inflammation, apoptosis, and extracellular matrix degradation in chondrocyte-like ATDC5 cells by mTOR and NF-κB pathways. BMC Musculoskelet Disord. 2025; 26 (1): 331. DOI: 10.1186/s12891-025-08536-9.
28. Collins T, Alexander D, Barkatali B. Platelet-rich plasma: a narrative review. EFORT Open Rev. 2021; 6 (4): 225–35. DOI: 10.1302/2058-5241.6.200017.
29. Mishra Kanchan, Desai Pooja, Khanna Manish, Malhotra Sayesha. Photoactivated platelet-rich plasma (PA-PRP): A safe and effective treatment for musculoskeletal disorders. IP International Journal of Orthopaedic Rheumatology. 2025; 11: 71–75. DOI: 10.18231/j.ijor.25218.1765359797.
30. Bustin SA, Ruijter JM, van den Hoff MJB, Kubista M, Pfaffl MW, Shipley GL, et al. MIQE 2.0: Revision of the Minimum Information for Publication of Quantitative Real-Time PCR Experiments Guidelines. Clin Chem. 2025; 71 (6): 634–51. DOI: 10.1093/clinchem/hvaf043.
31. Videla-Jiménez P, Ruz F, López-Martín M. Research on box plot knowledge in statistical education: a systematic review of the literature. Eur J Psychol Educ. 2025; 40: 141. DOI: 10.1007/s10212-025-01048-z.
32. Livak KJ, Schmittgen TD. Analysis of relative gene expression data using real-time quantitative PCR and the 2(-Delta Delta C(T)) Method. Methods. 2001; 25 (4): 402–8. DOI: 10.1006/meth.2001.1262.
33. Raut RD, Chakraborty AK, Neogi T, Michael Albro, Brian Snyder, Thomas P. Schaer, et al. A multi-tissue human knee single-cell atlas identifies that osteoarthritis reduces regenerative tissue stem cells while increasing inflammatory pain macrophages. Commun Biol. 2025; 8: 1146. DOI: 10.1038/s42003-025-08586-8.
34. Mocanu V, Timofte DV, Zară-Dănceanu C-M, Labusca L, Obesity. Metabolic Syndrome, and Osteoarthritis Require Integrative Understanding and Management. Biomedicines. 2024; 12: 1262. DOI: 10.3390/biomedicines12061262.
35. Galicia-Canales BE, del Rocío Aguilar-Gaytán M, Álvarez-Pérez MA, Jarquín-Yáñez K, et al. Effect of peniocerol on human meniscal fibrochondrocyte inflammation induced by IL-1β and TNF-α through the NF-κB signaling pathway. Cellular and Molecular Biology. 2026; 72 (3): 36–44. DOI: 10.14715/cmb/2025.72.3.5.
36. Rikkers M, Dijkstra K, Terhaard BF, Admiraal J, Levato R, Malda J, et al. Platelet-Rich Plasma Does Not Inhibit Inflammation or Promote Regeneration in Human Osteoarthritic Chondrocytes In Vitro Despite Increased Proliferation. Cartilage. 2021; 13 (2_suppl): 991S–1003S. DOI: 10.1177/1947603520961162.
37. Zhao H, Zhu W, Mao W, Shen C. Platelet-rich plasma inhibits Adriamycin-induced inflammation via blocking the NF-κB pathway in articular chondrocytes. Mol Med. 2021; 27 (1): 66. DOI: 10.1186/s10020-021-00314-2.
38. O'Donnell C, Migliore E, Grandi FC, et al. Platelet-Rich Plasma (PRP) From Older Males With Knee Osteoarthritis Depresses Chondrocyte Metabolism and Upregulates Inflammation. J Orthop Res. 2019; 37: 1760–70. DOI: 10.1002/jor.24322.
39. Li M, Jing C, Liu Q, Zhang Y, Li K. Platelet-rich plasma in cartilage repair: biological mechanisms and clinical perspectives. Front Sports Act Living. 2026; 8: 1785754. DOI: 10.3389/fspor.2026.1785754.